Asymmetry in Kinesin Walking†

Qiang Shao and Yi Qin Gao*

Department of Chemistry, Texas A&M University, College Station, Texas 77845

Received November 16, 2006; Revised Manuscript Received May 25, 2007

ABSTRACT: Several lines of experimental evidence suggest that the conventional kinesin 1 walks by an asymmetric hand-over-hand mechanism, although it is a homodimer. In the previous study, we examined several important force-dependent features of the hand-over-hand mechanism of kinesin. In this study, we focus on the asymmetry in the hand-over-hand mechanism. We show that the experimentally observed kinesin limping can be explained in our model by the variation of the neck linker lengths in the kinesin stepping (which has also been suggested earlier by others). We also study the experimentally observed processive motion of a mutant heterodimer of kinesin, in which only one of the two heads has the capability of ATP hydrolysis, as well as the walking of wild-type kinesin in the presence of both ATP and its analogue AMPPNP. We show that the possible processive walking of the heterodimeric kinesin can be explained by introducing a force-generating intermediate, the kinesin−ATP complex, which is different from the posthydrolytic species, kinesin−ADP/P_i.

Conventional kinesin is a microtubule-based linear protein motor. Because of its important biological functions in cargo transportation, cell division, and signal transduction, as well as its relatively small size compared to other linear motors, e.g., myosin and dynein, kinesin is among the most studied molecular motors (*1*−*3*). As a result of extensive structural, biochemical, and single-molecule studies, our understanding of kinesin as a motor has advanced dramatically over the past two decades, although many fundamental questions remain unanswered. Experiments have shown that the mechanical steps of kinesin are tightly coupled to the chemical transitions (*4*, *5*). However, the cooperativity between the two kinesin heads is not fully characterized. Although it is believed that the neck linkers connected to the kinesin heads may play a role as the lever arm and mediate the interaction between the heads, how the chemical state (e.g., different nucleotide occupation state) of the kinesin head influences the docking of the lever arm has not been unambiguously determined (*2*, *3*).

Kinesin walks by a hand-over-hand mechanism (*1*−*3*). Using high-resolution single-molecule fluorescence measurement, it was found that during walking the displacement of each of the two heads of the homodimeric kinesin varies between 16 and 0 nm, and the two heads exchange leading and trailing positions with each 8 nm stepping of the kinesin center for each ATP[1] hydrolysis (*6*). The hand-over-hand mechanism requires highly cooperative motions of kinesin in which the two identical motor heads alternate their roles in catalytic reactions and in physical motions. In principle, the hand-over-hand mechanism of kinesin can be either symmetric or asymmetric. Due to the lack of a mirror symmetry and the fact that the central stalk is formed from a coiled coil, in symmetric walking each of the forward steps should accompany a 180° rotation of the central stalk. However, in the asymmetric walking mechanism, no rotation of the stalk region should occur, and as a result, the steps differ depending on which head takes the leading position. The experiment of Hua et al. (*7*) showed that kinesin walks in the absence of the rotation of the central stalk. Combined with the later results which showed that kinesin walks by a hand-over-hand mechanism (*6*), this experimental observation indicates that kinesin walks by an asymmetric mechanism, although the experiment of ref *7* itself could not distinguish between an asymmetric hand-over-hand mechanism and an inchworm mechanism.

The asymmetry in the hand-over-hand mechanism, in the sense that every two consecutive forward steps are different, was confirmed by other experiments in which several kinesins limp during walking. In one of the experiments (*8*), a single amino acid mutation in the P-loop (nucleotide binding domain) of *Drosophila* kinesin caused ADP release to be ∼3.6-fold faster and the gliding velocity to be 3.3-fold slower. At low forces and/or low ATP concentrations, successive 8 nm steps were observed. However, at high forces and high ATP concentrations, one observed 16 nm steps. A careful analysis showed that the 16 nm steps are actually rapid double 8 nm steps. The 16 nm steps are thus due to alternating long and short dwell times. In another experiment, the wild-type kinesin, but with a truncated stalk, also exhibited significant limping behavior (*9*). It was shown in this experiment that the extent of limping increases when the central stalk is further shortened. The observed limping of kinesin suggests that in the stepping of kinesin, the two heads play different roles (which may not be evident for a

† We thank the ACS-PRF (44477-G6) and the Camille and Henry Dryfus Foundation for their support. For the computations in this paper, we used the Tensor Cluster at Texas A&M University, purchased with NSF Grant DMS0216275. Y.-q.G. is a 2006 Searle Scholar.

* To whom correspondence should be addressed. Telephone: (979) 458-0592. Fax: (979) 845-4719. E-mail: yiqin@mail.chem.tamu.edu.

[1] Abbreviations: ATP, adenosine triphosphate; ADP, adenosine diphosphate; P_i, inorganic phosphate; AMPPNP, adenyl-5′-yl imidodiphosphate.

10.1021/bi602382w CCC: $37.00
Published on Web 07/14/2007

wild-type kinesin walking under a low external load), and the walking is intrinsically asymmetric.

In yet another experiment (*10*), the ATP hydrolysis activity of the kinesin head was depleted to a large extent through mutation so that the ATP hydrolysis by the mutated kinesin head is at least 700 times slower than that by the wild type (*11*). The resulting homodimeric kinesin mutant does not walk along the microtubule processively. However, the mutation on only one kinesin head does not demolish the heterodimeric kinesin walking entirely, although the speed of kinesin was reduced by a factor of ~9 (*10*). This observation is surprising and poses serious challenges to the current understanding of the hand-over-hand mechanism. One of the possible explanations of the observation described above is that only one of the two heads plays a dominant role in driving the motion and the other plays only an assisting role. In this picture, the two heads are intrinsically nonequivalent, which is inconsistent with the experimental observations that the two heads are chemically equivalent (*2*, *3*, *6*). The other possibility is that during stepping there exists some kind of rescue mechanism due to the cooperation between the two heads; namely, the mutant head regains some ATP hydrolysis capability when fused with another wild-type kinesin head. On the other hand, an earlier experiment (*12*) showed that a single-headed kinesin fused with a different protein, which does not have ATP hydrolysis activity at all but does bind to microtubules, also walks processively along the microtubule, although at a slower speed. This experimental observation may suggest that without a rescue mechanism, a kinesin with a single motor domain maintains at least partial function. In this paper, we try to model the stepping of such a mutant kinesin as well as the stepping of the wild-type kinesin in the presence of both ATP and AMPPNP, with the hope of finding possible explanations for the experiments mentioned above.

A number of theoretical models for the mechanism of kinesin have been suggested, and the approaches that were used in these calculations include both kinetic modeling and master equation simulations, such as in refs *13*−*15*, just to name a few. In an earlier paper (*16*), we focused on the chemical and mechanical properties of wild-type kinesins and applied a simple model, in which ligand binding or release induces the conformational changes of the neck linker region with respect to the motor domain, to study the walking mechanism of kinesin. The model reproduces the hand-over-hand mechanism for kinesin walking in a large range of external loads. When a large force is applied in the minus direction, kinesin walks backward, again in a hand-over-hand fashion with 8 nm steps. The model was also used to explain the experimental results on the external force and the ATP concentration dependence of the walking velocity, the forward/backward step ratio, and the dwell times for both forward and backward steps. In the earlier paper, asymmetry during kinesin walking was included by assuming that the lengths of the neck linkers are dependent on which kinesin head takes the leading position. This difference in the lengths of neck linkers was not seen to induce asymmetry in the wild-type kinesin model (with relatively long neck linkers) even in the presence of a large external load.

In this study, we try to understand the experimental results for the two reconstructed kinesins, the one with a truncated stalk which limps during walking (*9*) and the one with a single functional ATP hydrolysis domain (*10*) (or a wild-type kinesin walking in the presence of both ATP and AMPPNP). We focus on the asymmetry in kinesin walking. The model is then used to make further predictions about the force dependence of the walking speed, the forward/backward stepping ratio, and the dwell times for these kinesin constructs. In particular, we examine in the model how the shortening of the neck linkers, and the reduction of the ATP hydrolysis activity of one of the two motor domains, compared to that used in the model for the wild-type kinesin, influence the chemomechanical coupling mechanism of this motor protein and induce limping during its walking.

It is worth noting here that the current model focuses on the walking patterns of kinesin under different conditions and does not focus on the processivity. A detached state of kinesin with both of its heads occupied by ADP is not involved. However, without detaching from the microtubule, a kinesin can still be "nonprocessive" by either not moving or moving without directionality or randomly. In some sense, it also describes the pattern of the processive motion of kinesin, although not the run length.

THEORETICAL MODEL

The model of kinesin presented here is based on the earlier study (*16*) (see Scheme 1 of the kinesin hand-over-hand forward/backward stepping mechanism), and the potential source of the asymmetry of kinesin walking is depicted in Scheme 1. In summary, the stepping of each of the two kinesin heads is described by the change in its position on the microtubule. The two heads are connected through their interaction in the neck linker region. The binding between each head and the microtubule is regulated by its chemical state. The chemical state determines the conformation between the head domain and its neck linker domain and therefore is coupled to the binding and motion of the other head. Kinesin at different chemical states binds the microtubule with different affinities: the binding affinity is the largest for the posthydrolytic ADP/P_i state; the ATP state and the empty state, on the basis of detachment experiments (*17*, *18*), are assumed to have similar but smaller binding affinities; the ADP state of kinesin head binds the microtubule most weakly. The main assumption of the model is, as mentioned earlier, that the ATP (or AMPPNP) binding induces a conformational change in the front kinesin head and thus provides a driving force in the plus direction (*19*). It is further assumed in this model that the hydrolysis of ATP to ADP/P_i generates an additional driving force for the motion of kinesin, even though this force could be significantly smaller than that due to ATP binding and the ATP- and ADP/P_i-bound states take similar stable conformations. A conformational change due to the hydrolysis of ATP has been suggested by fluorescence polarization experiment (*20*), which showed that the posthydrolysis state (mimicked by ADP·AlF_4^-) tends to be more rigid than the prehydrolysis state (AMPPNP-bound), in particular for a monomeric kinesin (*21*). The prehydrolytic state, in accordance with experiments (*20*, *21*), is assumed to bind microtubules more weakly than the posthydrolytic state. This assumption does not affect the results on the wild-type kinesin, the hydrolysis of ATP by which is fast enough for the population of the prehydrolytic state to be neglected; however, it does have an influence when the hydrolysis of ATP is missing, either

Scheme 1: (A) Schematic Diagram Showing the Effects of the Shortened Neck Linkers[a] and (B) Graphic Depiction of the Triangle Formed between Two Neck Linkers and the Microtubule[b]

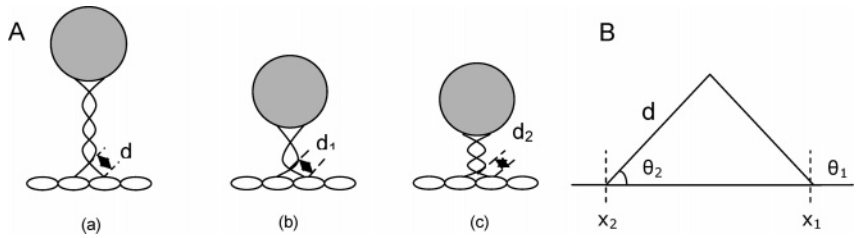

[a] (a) Wild-type kinesin. (b) Kinesin with a shortened neck linker due to the truncation of the coiled coil. In this paper, we postulate that the attachment of the top of the coiled coil to the bead exerts forces on it and perturbs the structure of the coiled coil at the top, e.g., relaxing or separating the two α-helices at this end. This perturbation of the protein structure is further expected to be transmitted along the coiled coil. For the shortened coiled coil, due to its internal rigidity, the perturbation is more likely to have a strong influence on the structure at the bottom, e.g., the interaction between two α-helices here being stronger to compensate for the destabilization at the top of the coiled coil, and thus lead to shorter neck linkers, whereas for wild-type kinesin, the long coiled coil is easy to relax to its native structure at its bottom. Therefore, d_1 is shorter than d. (c) Further shortening of neck linkers due to rewinding of the coiled coil. The effects of the rewinding and unwinding of the coiled coil on the binding conformations of kinesin heads are larger for the truncated kinesin as a result of its intrinsically shorter neck linkers ($d_2 < d_1 < d$). The scheme is not shown to scale. [b]The angle formed between the neck linker and microtubule is a function of leg length d and relative head position $x_1 - x_2$: $\cos\theta_1 = (x_2 - x_1)/2d$, and $\theta_2 = \pi - \theta_1$.

due to the lack of the ATPase activity of the catalytic core or due to the substitution of ATP with AMPPNP, in which the driving force due to ATP hydrolysis is absent. To take into account the two-step force-generating mechanism by ATP binding and hydrolysis, four possible chemical states are included for each kinesin head (ATP, ADP/P_i, ADP, and empty). [In the earlier study on wild-type kinesin (*16*), since ATP hydrolysis occurs fast, only three states were considered.] The ATP state is taken into account explicitly in the model presented here due to the lack of the hydrolysis of AMPPNP or ATP by a mutant motor domain. The prehydrolytic ATP state is assumed to be the same as the AMPPNP state.

The prevailing speculation about the causation of the asymmetry in kinesin walking is that the central coiled-coil stalk formed by the two kinesin monomers changes conformation during the stepping of the kinesin so that the lower portion of the coiled coil goes through unwinding and rewinding cycles, depending on which head is taking the leading position (*1*). As a result, the length of the neck linkers varies with the exchange of the head positions, although the neck linkers from the two kinesin heads always have equal lengths (so that the lengths of the two neck linkers change simultaneously during kinesin walking). This change in neck linker length is included in our simplified model by the change of the "leg length" parameter d (see Scheme 1, the total length from the lower end of the coiled coil to the head/microtubule binding site), which is 5.2 nm in the unwound state and 4.7 nm in the rewound state of the coiled coil of a wild-type kinesin (*16*); the changes in the lengths of the two neck linkers sum to ~1 nm, the approximate length of one repeat of the coiled coil (*9*). As we mentioned above, this length change (between 5.2 and 4.7 nm) has little influence on the walking of the wild-type kinesin, and there is no obvious "limping" at all tested external loads. We construct a similar model for a truncated kinesin, the upper portion of the coiled-coil stalk of which is shortened. This shortened central stalk is thought to make the lower end of the stalk wrap further (see a more detailed explanation in Scheme 1), and consequently, the neck linkers become shorter (*9*). This length change in neck linkers is also expected to be dependent on how much the stalk is shortened: the more the stalk is shortened, the shorter the neck linkers (*9*). As suggested by Block and co-workers (*9*), the change in the neck linker length during the walking of kinesin could also be a result of the switch between the registered and misregistered coiled coil near the neck region. In this study, due to the lack of detailed structural information, we do not distinguish between the possible origins for the change of the length of the neck linker during kinesin walking. In the model for the truncated kinesin, the value of d (for both unwound and rewound states) is smaller than that for wild-type kinesin (see results for the values of d). We note again that although the neck linkers are assumed to take different lengths depending on which head takes the leading position, the neck linker lengths of the two motor domains are always equal in length, changing simultaneously during kinesin stepping. The asymmetry of kinesin walking discussed in this paper refers to the difference between any two consecutive steps.

Once the model is constructed, simple potential energy functions are used to describe the interaction between each of the kinesin heads and the microtubule binding sites as well as that between the two kinesin heads (see the details in a previous portion of this section). The binding strengths used in our model are 9 kcal/mol for the ADP/P_i state, 7 kcal/mol for the ATP or empty state, and 4 kcal/mol for the ADP state. Given the chemical states of the two kinesin heads, the positions of the kinesin heads are then calculated using a master equation approach, including both diffusions of the motor heads along the microtubule and the chemical transitions of each head (*16*).

RESULTS

On the Limping of Kinesin. In the experiment of Block and co-workers (*9*), they observed that the truncation of the central stalk induces kinesin limping: during the kinesin walking, the dwell times consist of alternating short and long intervals. The limping factor L was defined as the ratio between the successive long and short dwell times for evaluation of the degree of limping (*9*). The experimentally observed relation between the truncation length and the limping factor (and dwell time) is very similar to the calculated neck linker length dependence of the limping factor in our model. Figure 1 demonstrates the influence of

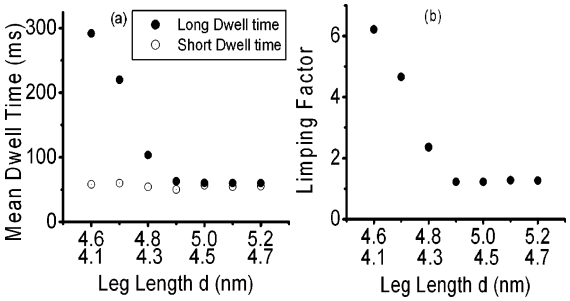

FIGURE 1: (a) Neck linker length dependence of the dwell times of the two kinesin heads. The filled and empty circles are for the longer and shorter dwell times, respectively. (b) Neck linker length dependence of the limping factor of kinesin. $F_{ext} = 4$ pN, and [ATP] = 2 mM. The other parameters used besides the neck linker lengths are given in Table 1.

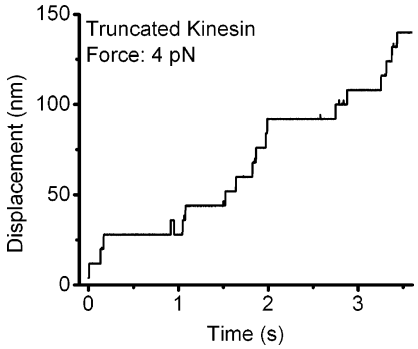

FIGURE 2: Trajectory of the center of a kinesin with neck linkers of 4.6 and 4.1 nm in the presence of a hindering force of 4 pN. [ATP] = 1 mM.

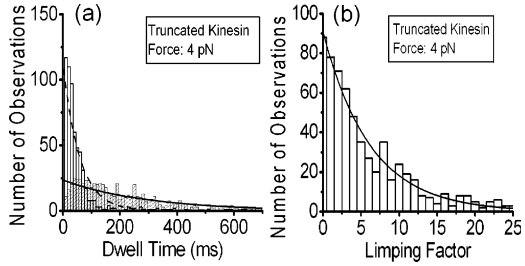

FIGURE 3: (a) Dwell times of the two kinesin heads. The empty and filled bars are for the fast and slow steps, respectively. (b) Distribution of the limping factor for a kinesin with neck linkers of 4.6 and 4.1 nm. $F_{ext} = 4$ pN, and [ATP] = 2 mM.

the neck linker length on the calculated limping factor as well as the dwell time: the mean long dwell time increases largely with the shortening of leg length *d*, whereas the mean short dwell time remains invariant (Figure 1a). As a result, the limping factor increases with the shortening of leg length *d* (Figure 1b). The calculated limping factor with neck linker lengths of 4.6 nm in the unwound state and 4.1 nm in the rewound state is similar to that obtained in the experiment for truncated kinesin DmK401, which has the shortest stalk in the series of tested kinesin constructs (see Figure 3B in ref *9*).

We calculated the trace of the center of the kinesin with the shorter neck linker lengths of 4.6 and 4.1 nm which is shown in Figure 2. One observes the alternating short and long intervals between forward steps. Figure 3a demonstrates the distribution of the long and short dwell times, and Figure 3b shows the distribution of the individual limping factor. As seen from the figures, there is a large difference

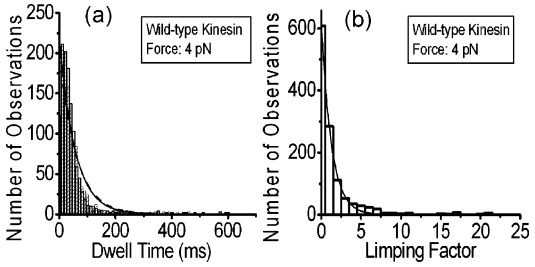

FIGURE 4: (a) Dwell times of the two kinesin heads. (b) Distribution of the limping factor for a wild-type kinesin (with neck linkers of 5.2 and 4.7 nm). $F_{ext} = 4$ pN, and [ATP] = 2 mM.

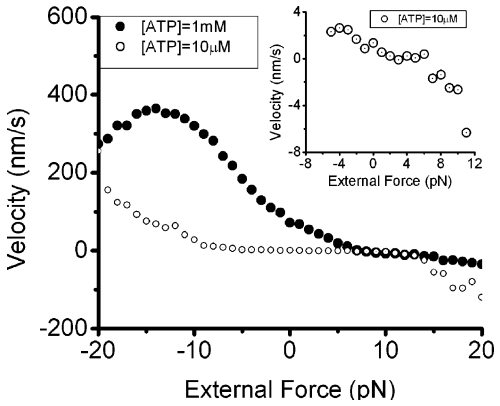

FIGURE 5: Predicted force dependence of the walking speed of the kinesin with neck linkers of 4.6 and 4.1 nm. An expansion of the figure in the force range of −8 to 12 pN is inserted to illuminate the small change in the walking speed of the kinesin with neck linkers of 4.6 and 4.1 nm under a small force. [ATP] = 10 μM.

between the dwell time distributions of the fast and slow phases. The mean dwell times for the slow and fast steps are as follows: $t_{slow} \approx 290$ ms and $t_{fast} \approx 58$ ms. The mean value of the limping factor L is ∼6.22. These values are consistent with the experimental results from Block and coworkers ($t_{slow} \approx 200$ ms, $t_{fast} \approx 40$ ms, and $L = 6.45 \pm 0.31$; see Figure 3B,C in ref *9*). As a comparison, one can see from Figure 4a that the dwell times of the fast and slow phases of wild-type kinesin (which as mentioned earlier has longer neck linkers) are very close: $t_{slow} \approx 56$ ms and $t_{fast} \approx 60$ ms. The corresponding mean value of the limping factor (Figure 4b) is ∼1.27, confirming that there is no limping during the walking of the wild-type kinesin.

We also calculated the walking speed of this kinesin with shorter neck linker lengths as a function of external force with 1 mM and 10 μM ATP. As shown in Figure 5, the force dependence of the walking speed of this kinesin is very similar to that of wild-type kinesin, although the speed of the former is slower. We calculated the limping factor under various external forces. As shown in Figure 6, kinesin limping becomes less severe at both large assisting and hindering forces, although the force at which the limping factor takes a maximum value depends on the system parameters (in particular the force dependence of the chemical reaction rate constants), and further experiments are needed to determine these parameters.

In addition, we calculated the average number of ATP molecules hydrolyzed per kinesin walking step to determine the chemomechanical coupling ratio. Figure 7 demonstrates the calculated coupling ratio under different forces. Over a large range of forces (from −15 to 12 pN for 1 mM ATP

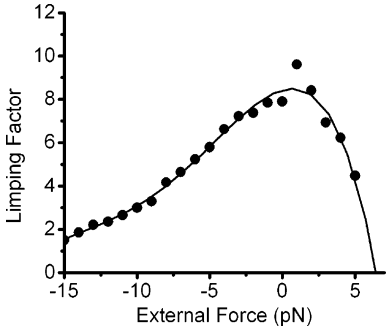

FIGURE 6: Predicted force dependence of the limping factor of the kinesin with neck linkers of 4.6 and 4.1 nm.

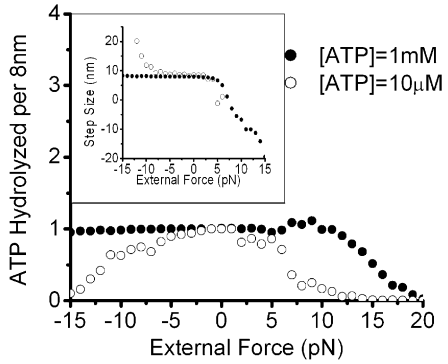

FIGURE 7: Predicted force dependence of the number of ATP molecules hydrolyzed per 8 nm movement of the kinesin with neck linkers of 4.6 and 4.1 nm.

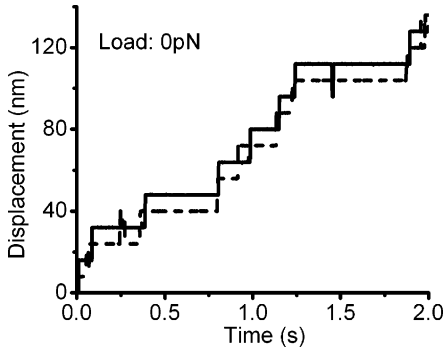

FIGURE 8: Trajectory for the motion of the two heads of the heterodimeric kinesin in the absence of an external load. [ATP] = 1 mM.

and from −5 to 5 pN for 10 μM ATP), the coupling ratio is close to unity, which means only one ATP molecule is consumed for each 8 nm step. Out of the force range mentioned above, the ratio decreases with an increase in the magnitude of the external force, corresponding to the sliding of kinesin induced by large external forces.

Heterogeneously Constructed Kinesin. In Figure 8, a typical trajectory is shown for the walking of a mutant kinesin, for which the hydrolysis activity of one of the two heads is removed, in the absence of external force. It is a hand-over-hand motion: during each step, one head moves 16 nm while the other head keeps attached to the microtubule, the same as during the stepping of a wild-type kinesin. The speed of the mutant kinesin obtained at a saturating ATP concentration of 1 mM is ~80 nm/s, which is ~6-fold slower than that of the wild-type homodimer (~450 nm/s).[2] This result is consistent with the experimental data of Thoresen and Gelles. A biotinylated *Drosophila* kinesin construct (K401-BIO-H6) with a switch I domain point mutation walks with a speed of ~90.3 nm/s (*10*) at 1 mM ATP. Limping is easily observed from the trajectories (the dwell times consist of alternating long and short ones), although this limping occurs via a mechanism that is different from that of kinesin with shortened neck linkers.

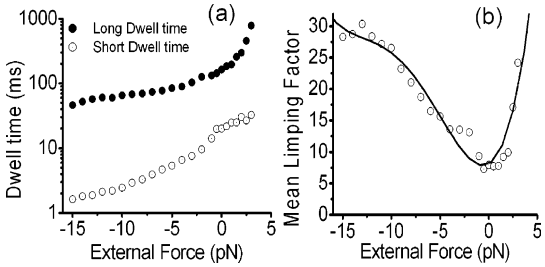

FIGURE 9: (a) Predicted force dependence of the average long and short dwell times of the heterodimeric kinesin with 1 mM ATP. (b) Predicted force dependence of the limping factor.

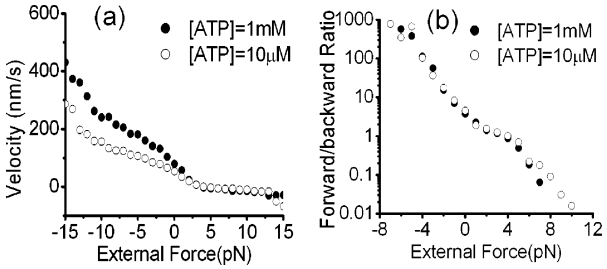

FIGURE 10: (a) Predicted force dependence of the walking speed of the heterodimeric kinesin, with 1 mM ATP (●) and 10 μM ATP (○). (b) Predicted force dependence of the forward/backward step ratio of the heterodimeric kinesin.

We calculated the mean values of the long and short dwell times as well as the limping factor of the mutant heterodimeric kinesin under various external forces. One can observe from Figure 9a that the increase in the hindering force prolongs the mean dwell time of both fast and slow phases, whereas an assisting force makes the dwell times in both phases shorter. The hindering force has a stronger influence on the long dwell time, while the assisting force affects more significantly the short dwell time. As a result, the difference between the long and short dwell times and the limping factor (the ratio of the mean value of long and short dwell time) reaches its minimum at around 0 force (as shown in Figure 9b).

The predicted force dependence of the walking speed of the mutant kinesin is shown in Figure 10a. The mutant and wild-type kinesins differ in that the speed of the former increases monotonically with the assisting force, while the

[2] The experiment of Gelles et al. used a short kinesin mutant, K401-BIO-H6. To compare with the experimental data, we also studied the walking of a heterodimeric mutant kinesin with the truncated stalk. We also calculated the velocity of a kinesin mutant with an intact stalk. We found that the neck linker length has little influence on the speed of the mutant kinesin if during the kinesin walking, the intact head takes the front position and the coiled coil is unwound (longer neck linkers of 4.6 nm). On the other hand, if the intact head is in the front while the coiled coil is rewound, the shortening of the neck linker (with a length of 4.1 nm) restricts the occurrence of the chemical transitions on the intact head (e.g., ATP binding). As a result, the speed of the mutant kinesin is largely reduced (~0 nm/s).

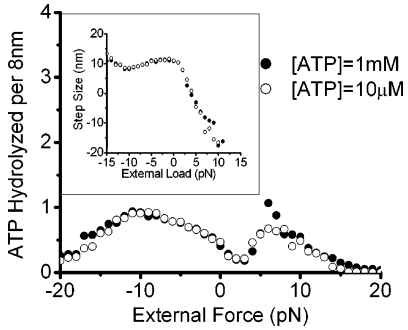

FIGURE 11: Predicted force dependence of the number of ATP molecules hydrolyzed per 8 nm movement of the heterodimeric kinesin.

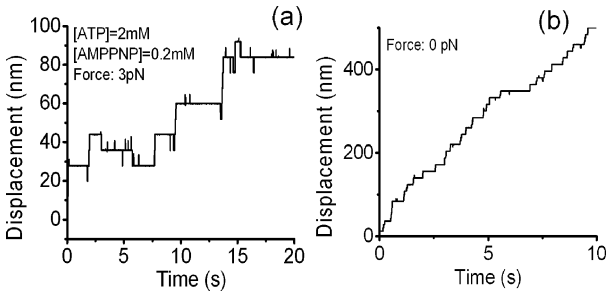

FIGURE 12: Typical trajectory of the motion of wild-type kinesin in the presence of 2 mM ATP and 0.2 mM AMPPNP in the presence of a load of 3 pN (a) and in the absence of any load (b).

latter has a maximum speed at approximately −5 pN (*16*, *22*). Figure 10b shows the force dependence of the forward/backward step ratio at ATP concentrations of 1 mM and 10 μM. As seen from this figure, the influence of the ATP concentration on the forward/backward ratio is very small, and in both cases, the ratio decreases monotonically with external force. The ratio becomes unity when the force is ∼3.5 pN, corresponding to a stall force that is approximately half of that of wild-type kinesin.

We also calculated the mean value of the number of ATP molecules consumed for each mutant kinesin step. As seen from Figure 11, the number of ATP molecules hydrolyzed per 8 nm step is ∼0.5 under near vanishing forces, in accordance with the fact that ATP hydrolysis occurs in only one head and the observation that the hydrolysis of one ATP couples to a forward step of each of the two heads.

Stepping of Wild-Type Kinesin in the Presence of both ATP and AMPPNP. We calculated the motion of the kinesin in the presence of 2 mM ATP and 0.2 mM AMPPNP. A segment of the trajectory for the motion of the center of kinesin is shown in Figure 12. The trajectories given in that figure were obtained in the absence and presence of a 3 pN hindering force, respectively. It is seen clearly that in the presence of the hindering force (Figure 12a), the kinesin frequently takes long pauses. These long pauses are normally terminated by a quick backward step, which is followed by either another segment of long pause or forward steps. The average waiting time before those backward steps is ∼3 s. On the other hand, the long pause during the processive motion of the kinesin appears rarely at small external forces (as shown in Figure 12b). These calculated results are again consistent with experiments (*23*). It was observed that in the presence of both ATP and AMPPNP, the wild-type kinesin still walks processively. However, under a hindering force (∼5 pN), the processive forward movement is halted frequently by long waiting periods and the forward motion is reactivated by an obligatory backward step.

The long waiting period, in our model, is induced by a state of the kinesin in which the front head is occupied by ATP or ADP/P_i, and the rear head is occupied by AMPPNP. As we assume in the model, the ATP binding as well as the following ATP hydrolysis in the front head supplies a driving force. The rear head which is bound with AMPPNP is detached from the microtubule and pulled forward if no external hindering force is applied on the kinesin, due to the stronger binding and larger driving force generated by ATP binding and hydrolysis in the other head. On the other hand, a large hindering force will balance the forward driving force on the rear head and therefore prohibit the rear head from moving forward. This stalled state survives a long time until the front head is drawn backward under the hindering force. Therefore, the two heads switch the leading position. The AMPPNP on the new front head is now released. If ATP binds to the head, kinesin resumes walking forward: the hydrolysis product P_i in the new rear head is released, and the ADP-bound head is easily detached from the microtubule under the driving force generated by the ATP-bound front head. However, if AMPPNP binds instead, the kinesin will be able to take one single forward step and then go back to the stalled state with an AMPPNP bound to the rear head.

DISCUSSION

In this study, we investigated the walking mechanism of kinesin and focused on the asymmetry in its hand-over-hand mechanism. We studied the processive walking of two reconstructed kinesins. The first is a kinesin homodimer with shorter neck linkers (used as a possible model for the kinesin with a truncated stalk) and the second a kinesin heterodimer, one head of which is deprived of ATP hydrolysis activity, although it does bind ATP. This model shows that both mutant kinesins limp during walking. For the kinesin with shorter neck linkers, Asbury et al. (*9*) speculated that the limping is due to the change in the neck linker length during the stepping of kinesin heads. As described in the asymmetric hand-over-hand mechanism, the lower portion of the coiled coil unwinds and rewinds in the successive steps. As a result, the conformations of the kinesin heads (represented in this model by the angles between the neck linker and the microtubule) are different depending on which head takes the front position. The chemical transitions, including ADP release, ATP binding, and ATP hydrolysis, are sensitive to the conformations of the kinesin heads. The neck linkers of a wild-type kinesin are long enough that the length change due to the unwinding or rewinding of the coiled coil has little influence on the conformations of its bound heads. On the other hand, the shortening of the central stalk is assumed to result in the shortening of the neck linkers, e.g., through misregistration of the coiled coil, by ∼1 nm (*9*). The shortened neck linker imposes more severe constraints on the conformations of the kinesin heads when they are bound to the microtubule (e.g., the angles between the neck linker and the microtubule deviate from their optimal values). The larger the deviation of the head conformation from its chemical transition conformation, the slower the chemical transition (see Scheme 1). As a result, the unwinding and

rewinding of the coiled coil have a more apparent effect on the chemical transitions with this shortened neck linker: Only when the central stalk unwinds does the kinesin conformation allow fast chemical transitions. The dwell time of wild-type kinesin is ~60 ms under a hindering force of 4 pN, while for the kinesin with shorter neck linkers under the same force, the dwell time is split into alterative fast and slow phases. The fast dell time (with an unwound coiled coil) is changed only slightly compared to the dwell time of wild-type kinesin, while the slow interval (with a misregistered coiled coil) becomes ~5 times longer. As mentioned earlier, the length of the neck linker (plus that of the kinesin head) is represented by the parameter *d*. Values of 5.2 and 4.7 nm were used for unwound and rewound wild-type kinesin, respectively. No limping is observed in the model with these two values. However, with the synchronous decrease in the two values, the limping becomes more and more evident (Figure 2). The limping factor reaches 6.22 with the values of 4.6 and 4.1 nm for a shortened kinesin, which is very close to the experimental value of kinesin DmK401 (*9*).

We use a construct similar to wild-type kinesin (*16*) to calculate the mutant kinesin with one head lacking the ability to hydrolyze ATP, which was also shown in our model to walk by the asymmetric hand-over-hand mechanism. Assuming that Head 1 does not hydrolyze ATP, we start with the prestroke state, in which Head 2 is occupied with ADP and Head 1 is empty. Head 1 takes the leading position. Binding of ATP to the front empty head (leads to an empty to ATP state transition) induces a conformational change in the neck linker and exerts a driving force that detaches the rear head and moves it forward. The difference between the mutant and wild-type kinesin is that Head 1 does not hydrolyze ATP and thus generates a smaller driving force [it is assumed in the model that in addition to ATP binding, the hydrolysis of ATP to ADP/P_i further provides driving force for kinesin walking, in accordance with fluorescence studies which show that ATP hydrolysis induces further kinesin conformational changes (*20*, *21*)]. Without a large hindering force, the rear head occupied by an ADP is easily detached from the microtubule and pulled forward by the front head. After Head 2 rebinds to its new microtubule binding site that is 16 nm from its previous binding site, ADP releases from it. The two heads have switched their leading positions. Although Head 1 does not hydrolyze ATP and binds the microtubule relatively strongly, ATP binding and hydrolysis in Head 2 generate a stronger binding state and a sufficiently large driving force to detach the ATP-occupied Head 1, and the competition between these two heads leads to a forward motion of the more weakly bound ATP-occupied rear head while Head 2 remains bound. This step is slower than the previous step as a result of the binding of an ATP (or AMPPNP)-occupied kinesin head that is much stronger than that of an ADP-occupied kinesin head to the microtubule. Consequently, the mutant kinesin limps when it walks. The resulting short dwell time corresponds to the first step: the front head is occupied by ATP, which remains in the prehydrolytic state, and the rear head is ADP-bound. The long dwell time, on the other hand, corresponds to the state in which the front head is occupied with the posthydrolytic ADP/P_i and the rear one is occupied by ATP. Because of the weak binding of the ADP-bound head to the microtubule, the assisting force will shorten the short dwell time more significantly than the long dwell time. The limping factor increases with an increase in the assisting force. On the other hand, the small hindering force has little influence on the short dwell time, whereas it aggravates the difficulty for the forward step to take place in the latter state. The limping factor also increases with the increase in hindering force.

It is seen from the description given above that the hydrolysis of one ATP molecule generates two successive 8 nm steps for a mutant kinesin. As a result, the stall force is smaller for a mutant kinesin (~3.5 pN) than for a wild-type kinesin (~7−8 pN) and the former walks slower than the latter. The smaller stall force and the slowness of the mutant kinesin could also be understood from the force-generating mechanism. In a wild-type kinesin, in every step a driving force generated from ATP binding and hydrolysis is used to detach the ADP-occupied kinesin head, while in a mutant kinesin, every other step the force is used to detach an ATP-occupied kinesin head, which is much more strongly bound to the microtubule.

The simple theoretical model we used for wild-type kinesin, kinesin with shorter neck linkers (*9*), and reconstructed kinesin heterodimers (*10*) provides possible explanations for the various experiments. As discussed above, although both the short neck linker homodimer and the mutant heterodimer exhibit limping behavior, the origins of limping are different. The chemomechanical coupling ratio of the short neck linker homodimer is the same as that of the wild type, and in the presence of small external forces, the hydrolysis of every ATP molecule leads to one 8 nm step whereas the consumption of one ATP molecule induces two consecutive 8 nm steps for the mutant heterodimer. The force dependence of motion, including the stall force of the kinesin with shorter neck linkers, is also similar to that of wild-type kinesin. Although both reconstructed kinesins walk at a similar speed in the absence of the external force, the heterodimer shows a much stronger force dependence and its stall force is only approximately one-half of that of wild-type kinesin and the kinesin with shorter neck linkers.

MODEL

Potential Energy Functions. In the simple model presented here, a dimeric kinesin contains two heads and a connection through the neck linkers. The two heads are represented by two points with their position given along the microtubule, which is represented by a single line. The two neck linkers, with always equal lengths, are connected through a connecting point which is determined by the length of the neck linkers [the distance between connecting point B and head positions A and A′ (see Scheme 1)]. Each of the two heads can bind the microtubule, with the binding sites separated by 8.1 nm on the line representing the microtubule. The binding between the kinesin head and the microtubule is represented by a simple function

$$V_b = V^s_{b,0}\left\{1 - \sum_i \exp\left[-\left(\frac{x - r_i}{a}\right)^2\right]\right\} \qquad (1)$$

In eq 1, $V^s_{b,0}$ and α are the depth and width of the binding potentials, respectively. The width of the binding potential is assumed to be independent of the chemical state of kinesin

Table 1: Parameter Values Used in This Study[a]

neck length d_1/d_2 (nm)	conventional kinesin	5.2/4.7 (unwinding state/ rewinding state)
	kinesin with shorter neck linkers	4.6/4.1 (unwinding state/ rewinding state)
kinesin−microtubule binding affinity (kcal/mol)	ATP-bound $V_{b,0}^{ATP}$	7.0
	empty $V_{b,0}^{E}$	7.0
	ADP/P_i-bound $V_{b,0}^{ADP/P_i}$	9.0
	ADP-bound $V_{b,0}^{ADP}$	4.0
chemical transition rate constant	ADP release (s^{-1})	260/2.6 (front head/rear head)
	ATP binding (μM^{-1} s^{-1})	3.0/0.3 (front head/rear head)
	ATP hydrolysis (s^{-1})	8.0/800.0 (front head/rear head)
	ATP release (s^{-1})	10.0
width of binding potential α (nm) (eq 1)		0.45/0.20 (forward/backward)
parameters in eq 2	internal force constant K_s (k_BT/nm^2)	0.047/0.04/0.031 (AD·PP_i/ ATP/empty state)
	$\Delta x_1(\Delta x_2)$ (nm)	−8.1 (ADP/P_i and ATP state) 8.1 (empty state)
overstretching potential V_0 (eq 3)		$10k_BT$
chemical transition constraint	chemically allowed range within binding site (nm)	0.16
	optimal neck linker angle	40°
	chemically allowed angle deviation for ATP binding	±5°
diffusion constant D (nm^2/s)		2.0×10^4

[a] The exact value of the stalk length is not used in this study. However, the stalk length change is the inverse of the neck linker length change during the kinesin walking: the longer the neck linker becomes, the shorter the stalk is.

(defined by its occupation, empty or occupied by ADP, ADP/P_i, or AMPPNP). The depth of the potential, thus the binding affinity, is dependent on the chemical state of the kinesin head; the $V_{b,0}^{s}$ values used in the present study are 4, 7, 7, and 9 kcal/mol for the ADP, empty, AMPPNP (or prehydrolytic ATP), and ADP/P_i states, respectively.

Besides the binding affinities, to take into account the conformation preference of kinesin at each of the chemical states listed above, the two heads are assumed to interact through the neck linkers, which are not necessarily rigid. The interactions between the two kinesin heads are again determined by the chemical states. The stable conformation between each head and its linkage is assumed in this model to be determined only by the chemical state of this head itself; thus, each head independently generates a potential as a function of the relative positions of the two heads, $x_1 - x_2$. Therefore, this interacting potential consists of two terms, one from each head. For the sake of simplicity, this interacting potential is taken to be a quadratic form and the stiffness of the potential is assumed to be proportional to the binding affinity between this kinesin head and the microtubule. In the ADP-occupied state, it is assumed that there is no orientation preference of the neck linkers, and thus, this energy term is absent for the ADP state. In contrast, the ADP/P_i or AMPPNP head prefers to be the rear head, so if this head has a position of x_1, a quadratic potential in the form of $^1/_2K_s(x_2 - x_1 - 8.1)^2$ is added to the total potential, with the force constant K_s given below.

The total potentials due to the conformational preference of the two heads are then

$$V_p = {}^1/_2K_{s,1}(x_1 - x_2 - \Delta x_1)^2 + {}^1/_2K_{s,2}(x_1 - x_2 - \Delta x_2)^2 \quad (2)$$

K_s is taken to be $0.047k_BT$, $0.04k_BT$, and $0.031k_BT$ nm^{-2} for the ADP/P_i, ATP, and empty states, respectively. Δx_1 and Δx_2 are determined by the chemical state of the kinesin head. For example, when Head 1 is empty, $\Delta x_1 = 8.1$ nm, and when it is occupied by ADP/P_i or ATP (AMPPNP), it is −8.1 nm.

In addition to the binding potential and the head conformation potential mentioned above, to include the excluded volume effect of the two heads and to avoid overstretching of the distance between the two heads, a potential of the form

$$V_{rep} = V_0\{\exp[(4 - |x_1 - x_2|)^2] + \exp[(|x_1 - x_2| - 9)^2]\} \quad (3)$$

is also included. V_0 is taken to be $10k_BT$.

Once the potential (the sum of the potentials in eqs 1−3) is specified, the force on each head is taken as the negative derivative of the potential over the position of the head (e.g., $-\partial V/\partial x_1$, for head 1), and the propagation for the motion of the head is performed using the Euler form of the Langevin equation (see the Supporting Information of ref *16*). The temperature was taken to be 298 K, and a value of 2×10^4 nm^2/s is used for the diffusion constant.

Chemical Transition Rate Constants and Their Force Dependence. The external force applied on kinesin inevitably results in the strain in the kinesin, which has an influence on the various chemical transitions (*3*). The force dependence of the chemical transitions is written in the present model as

$$k = k_0 \exp(-|F - F_0|\delta/k_BT) \quad (4)$$

δ/k_BT is taken to be ~2.5 pN^{-1} and F_0 is taken to be ~5 pN to yield a good fit to the experimental data on the force dependence of the kinesin speed, which shows a maximum at an external load (F_{ext}) of 5 pN. Since the force dependence of the binding affinities is not available, for the sake of simplicity, force-independent equilibrium constants are assumed in this study. Therefore, eq 4 is used for all chemical transition processes. A more elaborate model should take into account the difference in the force dependence of different rate processes. The values of rate constant k_0 of the various chemical transitions are taken from biochemical studies (*3*) and then slightly modified in this research to best fit the experimental data. To take into account the preference

of kinesin walking toward the plus end of the microtubule, we further assumed that the rate constants of the chemical transitions are not uniform on the two heads. The chemical transitions, e.g., ATP binding and ADP release, are much faster on the front head, whereas ATP hydrolysis occurs fast on the rear head instead of the front head. The rate constants used in this study are listed in Table 1.

In addition to the explicit force dependence, the chemical transition is also affected by the conformation of kinesin heads, represented here by the angle between the neck linker and microtubule and the distance between the kinesin head and its binding site on the microtubule. Chemical transitions are only allowed when the corresponding kinesin head is within a certain distance (taken as the value of 0.16 nm in this paper) of a binding site and when the neck linker angle is close ($\pm 5°$) to the stable value of the reacting site. When the angle is more than $\pm 5°$ or the distance is greater than 0.16 nm from that of its stable conformation, the rate constant is decreased 100-fold, the exact values of which have a small influence on the final results. Since in this model the force and kinesin conformation dependence are the same for all reactions (forward and backward), the equilibrium constants are independent of force or the kinesin docking or binding mode (a more elaborate model should certainly take into account the variance of the equilibrium constants).

The transitions between chemical states are treated as random processes, and the probabilities for the transition occurrence are determined by the rate constants of the transitions.

In the earlier paper (*16*), a different model without assuming the explicit force dependence of the rate constant of eq 4 was also used. It was shown there that these two methods yielded similar results when appropriate parameters were chosen. The fundamental assumption here is that only when the motor domain takes an appropriate conformation (correctly docked with the neck linker and bound strongly to the microtubule) do the chemical reactions occur at an appreciable rate.

REFERENCES

1. Yildiz, A., and Selvin, P. R. (2005) Kinesin: Walking, crawling or sliding along? *Trends Cell Biol. 15*, 112−120.
2. Asbury, C. L. (2005) Kinesin: World's tiniest biped, *Curr. Opin. Cell Biol. 17*, 89−97.
3. Cross, R. A. (2004) The kinetic mechanism of kinesin, *Trends Biochem. Sci. 29*, 301−309.
4. Coy, D. L., Wagenbach, M., and Howard, J. (1999) Kinesin takes one 8-nm step for each ATP that it hydrolyzes, *J. Biol. Chem. 274*, 3667−3671.
5. Schnitzer, M. J., and Block, S. M. (1997) Kinesin hydrolyses one ATP per 8-nm step, *Nature 388*, 386−390.
6. Yildiz, A., Tomishige, M., Vale, R. D., and Selvin, P. R. (2004) Kinesin walks hand-over-hand, *Science 303*, 676−678.
7. Hua, W., Chung, J., and Gelles, J. (2002) Distinguishing inchworm and hand-over-hand processive kinesin movement by neck rotation measurements, *Science 295*, 844−848.
8. Higuchi, H., Bronner, C. E., Park, H. W., and Endow, S. A. (2004) Rapid double 8-nm steps by a kinesin mutant, *EMBO J. 23*, 2993−2999.
9. Asbury, C. L., Fehr, A. N., and Block, S. M. (2003) Kinesin moves by an asymmetric hand-over-hand mechanism, *Science 302*, 2130−2134.
10. Thoresen, T., and Gelles, J. (2004) Processive movement by a mutant kinesin heterodimer with only one active head, *Biophys. J. 86*, 409A.
11. Klumpp, L. M., Mackey, A. T., Farrell, C. M., Rosenberg, J. M., and Gilbert, S. P. (2003) A kinesin switch I arginine to lysine mutation rescues microtubule function, *J. Biol. Chem. 278*, 39059−39067.
12. Inoue, Y., Iwane, A. H., Miyai, T., Muto, E., and Yanagida, T. (2001) Motility of single one-headed kinesin molecules along microtubules. *Biophys. J. 81*, 2838−2850.
13. Fisher, M. E., and Kolomeisky, A. B. (2001) Simple mechanochemistry describes the dynamics of kinesin molecules, *Proc. Natl. Acad. Sci. U.S.A. 98*, 7748−7753.
14. Astumian, R. D. (2000) The role of thermal activation in motion and force generation by molecular motors, *Philos. Trans. R. Soc. London, Ser. B 355*, 511−522.
15. Peskin, C. S., and Oster, G. (1995) Coordinated hydrolysis explains the mechanical behavior of kinesin, *Biophys. J. 68*, 202S−211S.
16. Shao, Q., and Gao, Y. Q. (2006) On the hand-over-hand mechanism of kinesin, *Proc. Natl. Acad. Sci. U.S.A. 103*, 8072−8077.
17. Uemura, S., Kawaguchi, K., Yajima, J., Edamatsu, M., Toyoshima, Y. Y., and Ishiwata, S. (2002) Kinesin-microtubule binding depends on both nucleotide state and loading direction, *Proc. Natl. Acad. Sci. U.S.A. 99*, 5977−5981.
18. Kawaguchi, K., Uemura, S., and Ishiwata, S. (2003) Equilibrium and transition between single- and double-headed binding of kinesin as revealed by single-molecule mechanics, *Biophys. J. 84*, 1103−1113.
19. Rice, S., Lin, A. W., Safer, D., Hart, C. L., Naber, N., Carragher, B. O., Cain, S. M., Pechatnikova, E., Wilson-Kubalek, E. M., Whittaker, M., Pate, E., Cooke, R., Taylor, E. W., Milligan, R. A., and Vale, R. D. (1999) A structural change in the kinesin motor protein that drives motility, *Nature 402*, 778−784.
20. Asenjo, A. B., Krohn, N., and Sosa, H. (2003) Configuration of the two kinesin motor domains during ATP hydrolysis, *Nat. Struct. Biol. 10*, 836−842.
21. Asenjo, A. B., Weinberg, Y., and Sosa, H. (2006) Nucleotide binding and hydrolysis induces a disorder-order transition in the kinesin neck-linker region, *Nat. Struct. Mol. Biol. 13*, 648−654.
22. Carter, N. J., and Cross, R. A. (2005) Mechanics of the kinesin step, *Nature 435*, 308−312.
23. Guydosh, N. R., and Block, S. M. (2006) Backsteps induced by nucleotide analogs suggest the front head of kinesin is gated by strain, *Proc. Natl. Acad. Sci. U.S.A. 103*, 8054−8059

BI602382W